A Model of Gene-Environment Interaction Reveals Altered Mammary Gland Gene Expression and Increased Tumor Growth following Social Isolation

J. Bradley Williams[#1], **Diana Pang**[#1], **Bertha Delgado**[2,3], **Masha Kocherginsky**[4], **Maria Tretiakova**[2], **Thomas Krausz**[2], **Deng Pan**[1], **Jane He**[1], **Martha K. McClintock**[3], and **Suzanne D. Conzen**[1,3,5]

[1]Department of Medicine, The University of Chicago, Chicago, Illinois

[2]Department of Pathology, The University of Chicago, Chicago, Illinois

[3]The Institute of Mind and Biology, The University of Chicago, Chicago, Illinois

[4]Department of Health Studies, The University of Chicago, Chicago, Illinois

[5]Ben May Department for Cancer Research, The University of Chicago, Chicago, Illinois

[#] These authors contributed equally to this work.

Abstract

Clinical studies have revealed that social support improves the outcome of cancer patients, whereas epidemiologic studies suggest that social isolation increases the risk of death associated with several chronic diseases. However, the precise molecular consequences of an unfavorable social environment have not been defined. To do so, robust, reproducible preclinical models are needed to study the mechanisms whereby an adverse environment affects gene expression and cancer biology. Because random assignment of inbred laboratory mice to well-defined social environments allows accurate and repeated measurements of behavioral and endocrine parameters, transgenic mice provide a preclinical framework with which to begin to determine gene-environment mechanisms. In this study, we found that female C3(1)/SV40 T-antigen mice deprived of social interaction from weaning exhibited increased expression of genes encoding key metabolic pathway enzymes in the premalignant mammary gland. Chronic social isolation was associated with up-regulated lipid synthesis and glycolytic pathway gene expression—both pathways are known to contribute to increased breast cancer growth. Consistent with the expression of metabolic genes in premalignant mammary tissue, isolated mice subsequently developed a significantly larger mammary gland tumors burden compared with group-housed mice. Endocrine evaluation confirmed that isolated mice developed a heightened corticosterone stress response compared with group-housed mice. Together, these transdisciplinary studies show for the first time that an adverse social environment is associated with altered mammary gland

Requests for reprints: Suzanne D. Conzen, The University of Chicago, 5841 South Maryland Avenue, MC 2115, Chicago, IL 60637. Phone: 773-834-2604; Fax: 773-834-0188; sdconzen@uchicago.edu..

Supplementary data for this article are available at Cancer Prevention Research Online (http://cancerprevres.aacrjournals.org/).

gene expression and tumor growth. Moreover, the identification of specific alterations in metabolic pathways gene expression favoring tumor growth suggests potential molecular biomarkers and/or targets (e.g., fatty acid synthesis) for preventive intervention in breast cancer.

The epidemiologic association between social environment, stress, and a variety of human pathologies, including cardiovascular disease and cancer, is well established (1–3). The underlying molecular mechanisms, however, are largely unknown. Because of the genetic and environmental variation in human populations, studying these underlying mechanisms is highly complex. Therefore, preclinical models are required to guide and refine hypothesis-driven clinical research questions. The recent discovery that mediators of neuroendocrine physiology [e.g., the β-adrenergic receptors 1 and 2 and glucocorticoid receptor (GR)] are expressed in breast (4, 5), ovarian (6), and prostate (7) cancer epithelium, as well as in diverse cell types of the surrounding stroma, provides evidence of potential physiologic connections between the (*a*) social environment, (*b*) neuroendocrine stress response, and (*c*) tumor gene expression and phenotype. An *in vivo* model to examine gene-environment interactions of such complexity requires a transdisciplinary approach that combines biobehavioral, endocrine, and tumor biology expertise. In turn, clinical and translational research might then examine the hypotheses suggested by preclinical animal data (8).

Despite the intriguing evidence supporting a connection between chronic social stressors and the natural history of human cancer, previous animal models have not combined biobehavioral, endocrine, and tumor biology expertise in a transdisciplinary approach. For example, although it is known from experiments using outbred mice that socially isolated males subjected to a superimposed acute stressor display significantly higher circulating corticosterone levels than group-housed animals (9), little is known about the consequences of the physiologic changes following social isolation on tumor growth in a well-validated genetically engineered mouse model of human cancer. Similarly, long-term socially isolated female Sprague-Dawley rats show increased corticosterone reactivity following exposure to an acute restraint stressor (10). A separate study that examined innate behavioral phenotypes showed that Sprague-Dawley female rats born with a relatively vigilant temperament develop earlier mammary gland tumors compared with innately social females (11). A follow-up study[6] revealed that isolated female rats exhibit both a higher corticosterone response to a restraint stressor and a greater likelihood of malignant versus benign mammary gland tumors. None of these models, however, have considered tissue gene expression changes and mammary gland pathology in conjunction with measuring the neuroendocrine stress response associated with a chronically adverse social environment.

In C3(1)/SV40 large T-antigen (Tag) mice, the C3(1) promoter fragment of the rat prostatic steroid binding protein gene is used to drive the gene encoding SV40 Tag. Unlike other commonly used transgenic promoters, including MMTV and WAP, the C3(1) fragment activity is not influenced by variations in stress-responsive hormones (described in this report) or estrogens (12). Based on the rodent biobehavioral literature, we predicted that female SV40 Tag mice subjected to chronic social isolation would develop measurable

---

[6]G.L. Hermes and M.K. McClintock, submitted for publication.

alterations in their corticosterone responses to everyday stressors (e.g., door openings, cage changes, mammary gland palpation, and tumor measurements). Furthermore, we hypothesized that these endocrine changes would be accompanied by changes in mammary gland gene expression and, potentially, with subsequent differences in mammary tumor growth. To test this hypothesis, following weaning, female SV40 Tag mice were assigned to markedly different social conditions. One cohort was housed in groups of four female mice, whereas the other cohort contained individually housed mice deprived of any interaction with other mice (social isolation). Repeated measures of mammary gland tumor size, gene expression, tumor differentiation, systemic corticosterone levels, and behavior were taken throughout the animals' life span. We observed significant differences in mammary gland tissue gene expression and subsequent tumor growth in the isolated versus group-housed animals. This *in vivo* model and the accompanying transdisciplinary approach together provide a new framework with which to begin to evaluate the molecular mechanisms whereby an adverse social environment may be associated with changes in breast cancer biology.

Materials and Methods

C3(1)/SV40 Tag transgenic mice

Female FVB/N mice homozygous for the SV40 large Tag gene driven by a fragment [C3(1)] of the rat prostatic steroid binding protein gene promoter were provided by the National Cancer Institute through the Mouse Models of Cancer Consortium.

Social environment

The University of Chicago Animal Care and National Institutes of Health guidelines were followed for all animal studies. Female offspring were weaned from their mothers at 3 wk of age and placed with their female siblings. Based on results from the open-field behavior test at 3.5 wk (inborn vigilance), balanced behavioral cohorts of female mice were divided into either socially isolated (single-housed) or group-housed environments. Details regarding separation of animals into housing environments are given below. Isolated cages measured $11 \times 6.5 \times 5$ in., and group-housed cages measured $15 \times 9 \times 9$ in. A 12-h light/dark cycle was maintained with lights out from 11:00 a.m. to 11: 00 p.m., so that mice were active during the investigators' measurements and their sleep cycle was not interrupted. Vaginal cytology was assessed daily in both groups to identify the length and periodicity of the estrous cycle. Of critical importance, all mice were sacrificed precisely 6 h into the dark cycle and during the estrus phase of the reproductive cycle to minimize experimental variability and to maximize interindividual reproducibility of gene expression.

Microarray analysis

Pectoral mammary glands from 15- and 20-wk-old group-housed and isolated mice were carefully dissected and immediately flash-frozen in liquid nitrogen ($n = 4$ each). Frozen mammary glands were thawed on ice and homogenized, and total RNA was isolated (RNeasy Mini Kit, Qiagen). RNA quality was assessed using an Agilent 2100 Bioanalyzer (Agilent Technologies), and concentration and 260:280 ratios (>1.8 for each sample was considered acceptable) were determined using an ND-1000 spectrophotometer (NanoDrop).

The Mouse Genome 430 2.0 Array GeneChip (Affymetrix) was used for global gene expression analysis.

Gene expression microarray data were normalized using the Robust Multiarray Average (RMA) algorithm (13) as implemented in the "affy" package in Bioconductor.[7] Differences in gene expression between isolated and group-housed animals' glands were assessed using Significance Analysis of Microarrays (SAM; ref. 14). In SAM, each gene i is assigned a score d_i that is proportional to the difference in expression between the two groups relative to the SD and is similar to the t statistic. Genes with scores exceeding adjustable cutoffs are called significant. These cutoff points are determined by selecting a threshold parameter so that the corresponding false discovery rate is at the desired level (e.g., 5%). In addition, fold changes >1.25 were required for a gene to be considered significantly up- or down-regulated. The SAM P values were determined based on permutations, and analyses were done using an R package "samr."[8] The gene expression data has been submitted to the Gene Expression Omnibus (*GEO*).[9]

Functional category assignment and pathway analyses of the RMA-normalized gene lists were then done using the Ingenuity Pathway Analysis (IPA) software (Ingenuity Systems 6.5).[10] The IPA P value represents the probability based on Fisher's exact test that each biological function assigned to the data set is due to chance alone. Significance scores of functional categories are given as $-\log_{10}(P)$.

We also compared murine genes with significant expression changes in the isolated versus group-housed mouse mammary glands with glucocorticoid-responsive genes identified in cultured human MDA-MB-231 breast cancer cells. MDA-MB-231 cells were serum starved for 48 h and then treated with dexamethasone (10^{-6} mol/L; versus vehicle). In the latter experiment, we used the Affymetrix human microarray HG-U133+2.0 to assess GR-associated gene expression at six time points from 30 min to 12.5 h following addition of dexamethasone. We next identified the human probes from the HG-U133+2.0 array that are orthologous to the mouse probes in the Mouse Genome 430 2.0 Array.[11] Mouse genes that had no available human orthologous probes were not further considered in the overlap analysis. The overlapping mouse and human genes with significant gene expression changes are listed in Supplementary Tables S3 and S4.

Quantitative real-time PCR

Pectoral mammary gland RNA was used in quantitative real-time reverse transcriptase-PCR (RT-PCR) assays to validate differences in gene expression from the gene expression arrays (15). Samples were run in technical triplicates; β-actin expression was used to normalize the RNA amount. Primer sequences were as follows: acetyl-CoA carboxylase α (*Acaca*), 5′-TACTGCCATCCCATGTGC-3′ (forward) and 5′-GCTTCCAGGAGCAGTCGT-3′ (reverse); ATP citrate lyase (*Acly*), 5′-AGCGATCCGAAGAGTTGG-3′ (forward) and 5′-

---

[7] http://bioconductor.org
[8] http://cran.r-project.org
[9] http://www.ncbi.nlm.nih.gov/geo
[10] http://www.ingenuity.com
[11] http://www.affymetrix.com/support/technical/byproduct.affx?product=moe430-20

GTTCTTTGCCGGTCTGCT-3′ (reverse); hexokinase 2 (*Hk2*), 5′-CTCCGGATGGGACAGAAC-3′ (forward) and 5′-TCGGCAATGTGGTCAAAC-3′ (reverse); and *β-actin*, 5′-GATATCGCTGCGCTGGTC-3′ (forward) and 5′-AATGGGGTACTTCAGGGTCA-3′ (reverse). Statistical analysis was done using the $2^{-\Delta\Delta Ct}$ approach as described in ref. (16). For each target gene, a mixed-effects ANOVA model was fitted with Ct as the response variable; housing type, gene type (target or reference), and housing $\times$ gene interaction as the fixed effects; and mouse as the random effect. A linear contrast was then constructed to estimate $\Delta\Delta Ct$ and its confidence interval, and the results were exponentiated to obtain the estimate of $2^{-\Delta\Delta Ct}$.

Tumor measurements

Beginning at 16 wk of age, the shortest and longest diameters of each tumor in all 10 mammary gland regions were measured weekly with electronic calipers. To maintain consistency in contact with the animals, caliper measurements were always done ~3 h into the dark cycle; that is, during the animal's awake period. Tumor volume was calculated using the formula for an ellipsoid sphere: (shortest diameter in mm)^2 $\times$ (longest diameter in mm) $\times$ 0.52. Tumors with volumes $\geq$ 200 mm^3 were used for comparative analysis because we found that measurement of smaller tumors was not consistent between two independent observers. Similarly, rare huge ("runaway") tumors that grew rapidly to >2,500 mm^3 before 20 wk of age were not used in the analysis. A mixed-effects ANOVA model was used to analyze differences in average tumor volume per mouse between isolated and group-housed animals. Tumor volume (the response variable) was log-transformed to satisfy the normality assumption, and the mouse random effect was included to account for the possible correlation between multiple tumors per animal. The mean tumor size on the original scale was then obtained based on the model estimates under the assumptions that tumor volume follows the log-normal distribution (17). The SEM was obtained based on the bootstrap distribution of the mean volume with $R = 1,000$ bootstrap samples. Mean $+/-$ SEM values are reported for this and other analyses unless otherwise noted.

Tissue processing and immunohistochemistry

Pectoral and inguinal mammary glands used for analysis were dissected immediately following sacrifice by CO_2 inhalation. The five right lateral mammary glands were rapidly harvested and then immediately individually flash-frozen in liquid nitrogen for subsequent RNA extraction. Left lateral mammary glands were then dissected and immediately formalin fixed, followed by paraffin embedding within 24 h. Paraffin-embedded 4-μm sections were stained using H&E or subjected to immunohistochemical analysis. Following antibody optimization, sections were prepared as described previously (18) and stained with the following antibodies: anti–estrogen receptor α (ERα; 1:100, Santa Cruz Biotechnology), anti–progesterone receptor (PR; 1:200, Lab Vision Corporation), anti-GR (1:200, Santa Cruz Biotechnology), anti-CD31 (1:200, Santa Cruz Biotechnology), anti-Ki67 (1:200, Lab Vision Corporation), and anti–cleaved caspase-3 (1:50, Biocare Medical).

To evaluate lung metastases, lungs were harvested immediately after sacrifice. Each right lung was fixed in formalin, whereas the left lung was immediately flash-frozen in liquid nitrogen. Formalin-fixed lungs were bisected from the apex to base and paraffin embedded.

Full-face histologic sections were stained with H&E and examined microscopically for evidence of tumor metastases by two pathologists (M.T. and T.K.).

Assessment of tumor differentiation

Paraffin-embedded mouse mammary glands were assessed for tumor morphology following the recommendations of the Annapolis Mouse Models Pathology Panel (19). A total of $n_T =$ 52 individual tumors from eight group-housed mice and $n_T = 62$ tumors from nine isolated mice were evaluated histologically for their degree of glandular differentiation. Mammary adenocarcinomas showing clear glandular or papillary formation in more than 75% of the largest cross-sectional area were classified as well differentiated. Adenocarcinomas in which glandular formation constituted between 10% and 75% of the total tumor area were classified as moderately differentiated, whereas those tumors exhibiting less than 10% glandular formation were classified as poorly differentiated. The difference in the number of tumors in each category between the group-housed and isolated mice was analyzed using a Poisson regression model.

Mammary intraepithelial neoplasia area, apoptosis, and proliferation indices

Mammary intraepithelial neoplasia (MIN) area analysis was done on contralateral mammary glands to those glands used for the microarray analysis at 15 wk of age. The largest cross-sectional area of the pectoral mammary gland fat pad ($n = 4$ mice for each cohort) was measured using the area assessment tool of a Leica laser microdissection microscope (Leica Microsystems). Following measurement of the total mammary gland area, the free-form tool was used to outline the area of all microscopically identified MIN in the largest diameter paraffin section of each mammary gland fat pad. The measured MIN area (including an occasional necrotic area in the center of a MIN region) within an individual mammary gland section was then divided by the total area of the corresponding mammary gland to calculate the relative percentage area of MIN.

The percentages of apoptotic and proliferating cells in MIN-involved mammary tissues were also determined in mice of 15 and 23 wk of age. These percentages were also determined in mammary adenocarcinomas from 23-wk-old mice. To measure apoptotic percentages, anti–cleaved caspase-3 antibody–positive epithelial cells in five randomly chosen fields (400× magnification) were calculated as a percentage of total cells counted (at least 2,000 cells were evaluated per section). Because apoptosis leads to nuclear fragmentation and decreased nuclear volume, this assay was done using traditional microscopy and manual counting to assess nuclear architecture as well as staining. Proliferation (the percentage of anti–Ki67-positive tumor cells) was calculated using the Automated Cellular Imaging System (ChromaVision) to determine the percentage of Ki67-positive nuclei relative to the total number of counterstained epithelial cells. For Ki67 staining, an area of at least 15,000 cells was examined at 100× magnification. The relative percentage of positively staining caspase-3 and Ki67 cells were compared between the two housing groups using the Wilcoxon rank-sum test.

Western analysis of SV40 Tag expression

To examine SV40 Tag expression levels in pectoral premalignant mammary glands (11-wk-old mice) and tumors (23-wk-old mice), tissues were rapidly harvested following CO_2 sacrifice, immediately flash-frozen, and stored at −80°C until Western analysis could be done. Protein extraction was done by rapidly weighing and pulverizing the flash-frozen tissues on a sheet of dry ice to prevent thawing. Pulverized tissues were incubated in extraction buffer (20 mmol/L Tris, 0.1 mol/L NaCl, 0.1 mmol/L EDTA) combined with a protease/proteasome/phosphatase inhibitor cocktail [1 mmol/L benzamidine, 40 mmol/L β-glycerol phosphate, 1 mmol/L phenylmethylsulfonylfluoride, 25 mmol/L NaF, 10 μmol/L ALLN, 10 μmol/L ALLM, 0.1 mmol/L sodium orthopervanadate, a protease inhibitor cocktail (Sigma), phosphatase inhibitor cocktail 1 (Sigma), protease inhibitor tablet (Roche), and 1% NP40] at a volume-to-mass ratio of 4:1 for 1 h at 4°C. Samples were vortexed briefly at 15-min intervals throughout the incubation. Homogenized tissues were then centrifuged at 3,500 rpm for 30 min at 4°C. The resulting supernatant was transferred to a new centrifuge tube, and protein content was determined using the Bradford assay (Bio-Rad). Samples were denatured at 95°C for 4 min in 2× Laemmli buffer (Bio-Rad), and 12.5 μg of total tumor protein and 30 μg of total mammary gland protein were resolved by SDS-PAGE. Equal loading of protein lysates and transfer to nitrocellulose was confirmed using Ponçeau red staining of the membrane. Following blocking with 5% skim milk TBS-T, blots were probed sequentially with either anti-Tag (1:200, Abcam PAb 416) or anti–β-actin (1:1,000, Sigma A5441) antibodies.

Corticosterone reactivity

To assess corticosterone reactivity to a well-validated rodent stressor, the serum from 22-wk-old mice was analyzed before and after a 30-min restraint (10). To ensure that any increase in corticosterone did not reflect underlying diurnal variation, the restraint period and serum sampling was initiated exactly 7 h into the 12-h dark cycle, which corresponds to the downward slope of the rodent diurnal corticosterone cycle (20). Mice ($n = 6$ group-housed, $n = 7$ isolated) were passively restrained within a ventilated 50-mL conical tube for 30 min. Blood samples were collected using the tail-nick method at baseline and 30, 60, and 120 min following initiation of the restraint. Whole blood (30 μL) was collected at each time point, placed immediately on ice, and centrifuged; serum was then stored at −20°C until analysis. The corticosterone assay was carried out using a double antibody RIA kit per the manufacturers' instructions (MP Biomedicals). Peak corticosterone levels following restraint were compared between group-housed and isolated mice using the Wilcoxon rank-sum test.

Behavior assessment

Three days after weaning, a baseline assessment of exploratory behavior was done using an open-field test. Specifically, each mouse (along with nesting material from her cage) was gently placed into a shallow plastic bowl (home base) that was positioned in the corner of a $4' \times 4'$ behavior apparatus resembling an open-field. The duration of time that passed before each mouse left its home base to enter the open-field was recorded. Based on results from this initial open-field behavior test, mice were divided into two cohorts (A and B) with a balanced distribution of behavior (i.e., a balanced distribution of the time until leaving home

base). Cohort A was then placed into group housing ($n = 36$, 4 mice per cage) and cohort B was placed into isolated housing ($n = 36$, 1 mouse per cage). Following 9.5 wk of differential housing, vigilance was reassessed. Time until entering the open field was compared between group-housed and isolated mice using the log-rank test. Times were censored at 300 s for mice who did not leave home base within 5 min.

Results

A model to evaluate mammary gland tumorigenesis following social isolation

By ~12 weeks, female C3(1)/SV40 Tag mice develop a preinvasive neoplasia termed MIN (21), making this an excellent model for studying the development of human breast cancer. In addition, unlike other transgenic models of human breast cancer that commonly use MMTV or WAP promoter-driven transgenes, the C3(1) promoter is not affected by estradiol (12). We first ensured that the neuroendocrine changes associated with chronic social isolation were not associated with altered C3(1)/SV40 Tag transgene expression by examining mammary gland protein extracts from 11-wk-old mice (Fig. 1A) and tumors from 23-wk-old mice (Fig. 1B) for differential SV40 Tag protein expression. Blots were probed with an anti-SV40 Tag or anti–β-actin antibody (as a loading control). Densitometric analysis showed that there were no significant differences in SV40 Tag expression in mammary glands from group-housed versus isolated mice.

Having observed no differences in SV40 Tag expression, we initiated experiments to determine whether social isolation is associated with altered mammary gland tumor development in this model. Figure 2 shows an outline of the experimental approach, which combined behavioral, endocrine, mammary gland gene expression, and tumor size measurements.

Socially isolated mice develop larger mammary gland tumors than group-housed mice

Mice subjected to chronic isolation from weaning until 21 weeks of age developed a greater number (n_T) of larger tumors ($n_T = 25$ versus $n_T = 11$) ranging in size from 600 to 2,500 mm^3 ($n = 26$ mice in each cohort; Fig. 3A), and a higher proportion of mice in isolated housing developed at least one of these large tumors (61.5% versus 30.8%, $P = 0.05$). At 21 weeks, when most mice had developed one or more palpable tumors (>200 mm^3), the average tumor size among the group-housed mice was 521.9 mm^3 ± 36.9 versus 792.2 mm^3 ± 67.3 ($P = 0.01$ by mixed effects ANOVA; Fig. 3B). At the same point, the overall tumor incidence (proportion of mice with at least one palpable tumor) was 21/26 (80.8%) in isolated mice versus 17/26 (65.4%) in group-housed mice ($P = 0.35$, Fisher's exact test). All palpable tumors were confirmed at necropsy to contain invasive carcinoma. Changes in per-mouse tumor burden (log transformed) over time are shown in Supplementary Fig. S1 and suggest that the rate of average tumor growth in the isolated mice cohort begins to increase significantly around 18 weeks of age, whereas the isolated tumor burden becomes significantly higher than the group-housed tumor burden by 21 weeks ($P = 0.01$).

Analyses of apoptosis and proliferation indices were conducted in both MIN (15 weeks) and invasive tumors (23 weeks). Although differences in the proportion of apoptotic (anti–

cleaved caspase-3 positive) or proliferative (anti-Ki67 positive) epithelial tumor cells were not statistically significant, we noticed a qualitative difference in invasive carcinoma morphology between the two groups. To more objectively assess this, we evaluated the degree of glandular differentiation of murine mammary carcinomas based on the nomenclature recommended in the Annapolis consensus report (19). Figure 3C shows a representative example of well-, moderately-, and poorly- differentiated adenocarcinomas that were categorized on the basis of their degree of glandular differentiation. An analysis of 114 adenocarcinomas from 17 mice, conducted by two pathologists who were not aware of the mouse's environment, showed a trend toward a higher number of poorly differentiated adenocarcinomas in the isolated mice ($P = 0.058$; Fig. 3D).

These data suggest that social isolation may be associated with the development of more poorly differentiated and larger mammary gland tumors in genetically identical mice. Because ERα can be associated with well-differentiated human breast cancers, we examined ERα and PR expression using immunohistochemistry of paraffin sections of normal-appearing mammary glands, MIN, and adenocarcinomas from both isolated and group-housed mice. This analysis revealed nuclear ERα and PR expression in mouse mammary gland luminal epithelial cells with normal morphology, but only in about 30% of MIN cells in both isolated and group-housed mice. Consistent with prior reports (12), ERα and PR expression was completely absent in all mammary gland adenocarcinomas (Supplementary Fig. S2), suggesting that neither ERα nor PR expression mediates the phenotypic differences seen between the two groups (data not shown). GR expression was observed with equal intensity in all adenocarcinomas from both grouped and isolated animals. Overall, these data suggest that the expression of these nuclear receptors did not differ significantly by housing group.

We hypothesized that differences in the natural history of tumor growth from group-housed versus isolated SV40 Tag mice might be initiated by biological differences at the *in situ* stage (MIN) of tumorigenesis. Microscopic examination of mammary glands from a subset of 15-week-old mice showed numerous lobules filled with neoplastic cells corresponding to preinvasive carcinoma (MIN; Fig. 4A). We calculated the percentage area of MIN in the largest cross section of a single mammary gland from isolated ($n = 4$) versus group-housed ($n = 4$) mice and found that, on average, the area involved by MIN was somewhat higher in the isolated versus group-housed mouse tumors (5.2% ± 1.4 versus 2.8% ± 0.5), although the difference was not statistically significant ($P = 0.25$; Fig. 4B).

In addition to analyzing *in situ* neoplasias, we also examined lungs from isolated and group-housed mice for evidence of gross and microscopic metastases. In two independent experiments, there was no evidence of gross metastatic disease in any of the lungs examined from either cohort. However, we found that 3 of 15 isolated (20%) versus 8 of 16 group-housed (50%) mice showed microscopic evidence of metastases to the lungs at 23 weeks of age ($P = 0.14$, Fisher's exact test). Therefore, in this model, there seemed to be no statistically significant difference in the incidence of metastases between isolated and group-housed mice.

Altered gene expression in mammary glands from isolated mice suggests activation of cancer-associated metabolic pathways

Because cancer development is a multistep process, we also examined gene expression changes in mammary glands from isolated versus group-housed mice at 15 weeks of age. We hypothesized that differences in the social environment might be associated with altered gene expression in the mammary glands because the social environment has been previously linked to significant gene expression changes in various tissues, including the central nervous system of mice (22) and the peripheral blood lymphocytes of humans (23). To examine gene expression differences, RNA was extracted from a subset of 15-week-old mammary glands (n = 4 mice in each group) that included some MIN but no invasive cancer or palpable tumors. Global steady-state mRNA levels were measured using Affymetrix technology and the Robust Multiarray Average (RMA) algorithm (13) was used for normalization. Using a false discovery rate of 5% and a minimum fold change of 1.25 (0.80 for down-regulation), 296 down-regulated (Supplementary Table S1) and 68 up-regulated transcripts (Supplementary Table S2) were identified in 15-week-old mouse mammary glands. We similarly examined mammary gland gene expression in mammary glands from mice that were 20 weeks old that contained no palpable tumors.

We next identified specific functional and disease categories using IPA[12] for the differentially expressed genes from isolated versus group-housed mice. Among the 15-week-old mice, we found that gene expression related to immunologic disease (P = 4.08E−09), inflammatory disease (P = 8.67E−09), and lipid metabolism (P = 2.73E−08) was significantly different in the isolated versus group-housed mouse mammary glands (Fig. 5B). Among the metabolic genes, significantly increased gene expression was identified in genes encoding three key enzymes known to be associated with cancer development: ATP citrate lyase (*Acly*), acetyl-CoA carboxyl ase α (*Acaca*), and hexokinase 2 (*Hk2*; refs. 24–27). The human orthologues of mouse *Acly* and *Acaca* were previously shown to be up-regulated in aggressive, metastatic breast cancer cell lines (30) and to be essential for breast cancer cell survival (27, 28), respectively. We therefore examined whether there was an increased expression of mouse *Acly, Acaca,* and *Hk2* mRNA by quantitative RT-PCR using individual mammary gland RNA from socially isolated versus grouped housed mice (Fig. 5A). This analysis confirmed a 1.5- to 3-fold increase in steady-state mRNA expression in mammary glands from isolated versus group-housed mice for all three metabolic pathway genes, suggesting that chronically isolated transgenic mice exhibit gene expression changes associated with increased glycolytic and lipogenic metabolic pathway activation (Fig. 5C). Interestingly, activation of these pathways has been postulated to be a precursor to tumor development in several cancer models (29, 30).

Using the same criteria, we examined gene expression differences in mammary glands without palpable tumors from 20-week-old mice. However, far fewer differences in gene expression were noted at the later time point: Using the same statistical criteria, only 6 down-regulated (Supplementary Table S5) and 18 differentially up-regulated transcripts (Supplementary Table S6) were identified in the mammary gland RNA from socially

---

[12]http://www.ingenuity.com

isolated versus group-housed older animals. In addition, no functional categories from pathway analysis met the stringent P value cutoff of 1×10^{-7} used for the 15-week-old mice. These findings suggest that in this genetically engineered mouse model of human breast cancer, significant differences in metabolic pathway gene expression associated with an altered social environment occurs in younger mice at the initial stages of carcinogenesis.

Isolated mice exhibit increased vigilance and higher corticosterone reactivity

The mechanisms connecting prolonged social isolation to gene expression changes have long been hypothesized to involve alterations in the neuroendocrine axis (i.e., epinephrine and corticosteroid responses). These changes are accompanied by distinct alterations in rodent behavior that can be measured by well-established behavior tests, such as the open-field test. We therefore wished to determine whether these transgenic mice exhibit differences in exploratory behavior when subjected to grouped or isolated environments (31, 32). We performed baseline open-field testing of mice at ~3 weeks of age before dividing them into two differentially housed groups (3.5 weeks; Fig. 6A). We used their initial exploratory behavior, measured as the number of seconds taken to leave the home base, to separate the mice into two balanced groups with similar overall behavioral profiles. Behavior of the same cohorts of mice was then reassessed following 9.5 weeks of differential housing. Following assignment to social isolation, SV40 Tag mice showed an overall significantly longer time to enter an open field (i.e., increased vigilance; $P = 0.018$ based on log-rank test; Fig. 6B). These observations were confirmed in two additional experiments and support the conclusion that social isolation has a reproducible and quantifiable behavioral effect on these inbred animals.

We next examined whether the isolated social environment favors a heightened endocrine stress response (e.g., increased corticosterone reactivity) by measuring serum corticosterone levels at baseline and following a moderate passive restraint. Figure 6C shows individual mouse corticosterone measurements relative to their respective baseline levels. No statistically significant differences were observed in the baseline corticosterone levels, suggesting that chronic isolation does not affect basal corticosterone levels in this model (Fig. 6D). However, the subset of isolated mice examined exhibited a significantly greater rate of increase in reactive serum corticosterone during passive restraint ($P = 0.022$ based on Wilcoxon rank-sum test; Fig. 6E). Furthermore, the peak absolute increase in serum corticosterone was significantly greater in the isolated mice compared with group-housed mice (74.5 μg/dL ± 10.8 versus 39.2 μg/dL ± 3.2, $P = 0.032$ based on Wilcoxon rank-sum test). These data suggest that chronic social isolation is associated with greater exposure to corticosterone in response to moderate restraint stressors, such as those that may be encountered during routine animal husbandry and tumor measurements.

Discussion

The availability of genetically engineered mouse models of cancer allows cancer biologists to study tumorigenesis under reproducible environmental conditions and to examine epigenetic changes in gene expression that may influence cancer progression. To investigate the potential role of social isolation in breast cancer and mammary gland gene expression,

we subjected SV40 Tag transgenic mice to significantly different social environments and found that isolation from other mice is associated with both an alteration in behavior and glucocorticoid reactivity to an acute stressor. Although we initially hypothesized that changes in mediators of the neuroendocrine axis (e.g., glucocorticoids and catecholamines) might result in a significant decrease in apoptosis and/or an increase in tumor cell proliferation, these differences did not reach statistical significance in this mouse model. It is possible that the highly transformed and proliferative SV40 Tag-driven mammary gland carcinomas develop too rapidly to detect significant differences in proliferation/apoptosis. While social isolation was not associated with a difference in the incidence of palpable tumors, we did, however, observe larger mammary tumors in the socially isolated transgenic mice. Furthermore, we observed increased expression of metabolic and lipid synthesis genes in the mammary glands from 15-week-old isolated versus group-housed mice before evidence of invasive carcinoma. The activation of both glycolysis and lipid synthesis pathways has previously been implicated in human breast cancer growth, a finding consistent with the subsequent development of a much larger tumor burden in isolated animals.

We speculate that the differences in mammary gland gene expression in isolated mice at 15 weeks favor the increased growth potential of a subset of MIN lesions that progress to invasive cancer. Recent magnetic resonance imaging (MRI) data from our group support this hypothesis by suggesting that only some SV40 Tag MIN lesions progress to invasive (and eventually palpable) tumors, whereas other MIN lesions remain stable in size or regress. In future studies, we will use these novel imaging techniques to accurately investigate whether stress-induced gene expression changes such as those we have identified can influence the likelihood of MIN lesions to progress to invasive carcinomas, in addition to causing the increased tumor growth that we saw in our present study.

Differential glucocorticoid (and/or catecholamine) stress reactivity may influence tumor development in the isolated SV40 Tag mouse through activation of their respective receptors and resultant downstream changes in gene expression. Previously, GR activation in human breast cancer xenograft models was shown to result in antiapoptotic signaling and increased cell survival (33, 34). In the SV40 Tag mouse model reported here, we observed a progressive increase in the percentage of GR-expressing tumor cells in mammary glands of mice of both housing conditions, raising the possibility that increased glucocorticoid hormone responsiveness observed in isolated mice might favor mammary tumor growth. Although we did not observe a specific difference in apoptosis in isolated versus group-housed mammary gland tumors, the effect of glucocorticoids on the early tumor environment cannot be ruled out. In addition, there is long-standing evidence that adrenergic receptors are present in human breast cancer cells (35), although to date these receptors have not been examined in genetically engineered mouse models of breast cancer.

Our studies also reveal that at 15 weeks of age, before mammary gland carcinomas are invasive, many more down-regulated genes (compared with up-regulated genes) were identified in the whole mammary glands from social isolates versus group-housed animals. Interestingly, in human subjects, perceived loneliness was also recently found to be associated with an overall greater down-regulation of gene expression in peripheral blood

leukocytes (131 down-regulated versus 78 up-regulated genes; ref. 23). Furthermore, in a transgenic mouse model of Alzheimer's disease, far more down-regulated ($n = 36$) than up-regulated ($n = 5$) transcripts were observed in the brains of animals housed in a stark versus an enriched environment (22). Taken together, these data suggest that a less enriched and interactive environment (e.g., social isolation) may be associated with globally repressive effects on gene expression. It is tempting to speculate that the increased physiologic responsiveness to a superimposed, acute stressor observed in the isolated mice may mediate epigenetic mechanisms of gene silencing through hormone action (36). Recently, a tissue culture model of chronic exposure to elevated concentrations of glucocorticoid in epithelial cells found clear evidence of chromatin remodeling and GR-mediated gene repression (37).

Despite predominantly down-regulated gene expression in the isolated mouse mammary glands, the whole genome mammary gland gene expression studies identified significantly elevated expression of the murine orthologues of three key metabolic genes that are known to play a role in human tumorigenesis: the cancer-associated glucose kinase, hexokinase 2 (*Hk2*), as well as the key lipogenic enzymes ATP citrate lyase (*Acly*) and acetyl-CoA carboxylase α (*Acaca*; Fig. 5C). *HK2*, the human orthologue of mouse *Hk2*, is overexpressed in many human cancers (38) and encodes a protein that catalyzes a critical step in the glycolytic pathway; that is, the phosphorylation of glucose to glucose-6-phosphate (39). Unlike other hexokinase isoforms, the activity of mitochondrial-bound HK2 is not inhibited by glucose-6-phosphate production (40). As Pedersen describes in his review of the Warburg effect (41), this lack of inhibition, along with the close proximity of HK2 to ATP synthesis at the inner mitochondrial membrane, allows HK2 to effectively "jump start" glycolysis. As a result, the glycolytic pathway accounts for a significant proportion of the cancerous cell energy production due to over-expression of HK2. In addition, the increased rate of glycolysis provides the premalignant or cancerous cells with many bio-synthetic precursors that are necessary for rapid proliferation. Importantly, the increased rate of glycolysis in tumor tissues is observed even in the presence of oxygen and is therefore not simply a result of reduced mitochondrial energy production in hypoxic conditions. It has also been shown that increased HK2 expression inhibits apoptosis through binding to the voltage-dependent anion channel and interfering with proapoptotic Bax activity (24). Therefore, the finding that murine *Hk2* expression is significantly increased in the premalignant mammary glands from isolated mice suggests that the social environment may be associated with subsequent tumor growth through changes in mammary gland gene expression. However, it is impossible to say with certainty whether the slightly increased percentage of MIN area in the mammary glands of isolated versus group-housed mice accounts for the significant differences in metabolic gene expression or whether instead the differences in gene expression result from differential gene regulation in preneoplastic mammary epithelium, the surrounding adipocytes and other stromal cells, or both.

Despite the increased glycolytic rate in cells exhibiting the Warburg effect, glycolysis accounts for no more than 50% of the total energy production of cancerous cells (41). The remainder of the energy is produced through the mitochondria. Interestingly, in isolated mammary glands, we also observed the increased expression of two important lipid synthesis pathway genes that encode enzymes that modify the mitochondrially produced

citric acid cycle intermediate, citrate, to precursors of lipogenesis (Fig. 5). The first, *Acly,* encodes the enzyme that converts citrate into cytosolic acetyl-CoA. *Acaca,* another up-regulated gene, encodes the enzyme required for conversion of acetyl-CoA to malonyl-CoA, the rate-determining step of lipogenesis (42). These CoA derivatives, in conjunction with products from the glycolytic pathway, provide important lipids necessary for enhanced tumor cell proliferation (43). Several *in vitro* and *in vivo* studies also suggest that increased lipid synthesis is linked to tumor growth. For example, human *ACL* expression (*ACL* is the human orthologue of the mouse *Acly* gene) is elevated in breast cancer cell lines compared with normal breast epithelial cell lines (28). Supporting evidence that lipid synthesis may be a targetable pathway for regulating tumor growth and possibly prevention comes from a study showing that knockdown of *ACL* expression suppresses lung adenocarcinoma cell growth (25).

Similar to *ACL,* human *ACC*α (orthologous to the mouse *Acaca* gene) expression is frequently elevated in breast carcinoma (44). Furthermore, down-regulation of ACCα leads to a significant increase in apoptosis in both MDA-MB-231 and MCF-7 breast cancer cell lines (27). Similarly, ACCα activity is essential for survival and proliferation of prostate cancer cell lines (45) and knockdown of ACCα leads to inhibition of prostate cancer cell proliferation (26). Interestingly, it has been suggested that the human breast cancer tumor suppressor protein BRCA1 may form a complex with phosphorylated ACCα, thereby maintaining ACCα in its phosphorylated/inactive state and reducing tumor cell growth (46). Some *BRCA1* deleterious mutations prevent the formation of the BRCA1/pACCα complex, thereby enabling the cell to enter a high-energy state that favors anabolic metabolism and supports tumor growth.

The increased expression of the important metabolic genes found in this study is consistent with the hypothesis that social isolation is associated with higher activity of important glycolytic and lipid synthesis pathways favoring tumor growth (Fig. 5). Conversely, increased social support might favor inhibition of these gene expression pathways, many of which are associated with lipid production. Recent clinical evidence supports the role of social support in reducing breast cancer growth—in a study of 227 early-stage breast cancer patients who were randomized to receive either social intervention or no additional social support following adjuvant chemotherapy, enhanced psychosocial support reduced the risk of breast cancer recurrence (hazard ratio, 0.55; $P = 0.034$) and death (hazard ratio, 0.44; $P = 0.016$; ref. 50).

The additional finding that many of the differentially regulated mammary gland genes from animals assigned to an isolated versus group-housed environment are composed of inflammatory, immunologic, as well as metabolic genes also suggests that differential glucocorticoid exposure may mediate some of the differences in gene expression. Interestingly, up-regulated *ACC*α mRNA expression (47, 48) and increased ACL activity (49) have been previously linked to GR signaling. To further explore the possibility of a glucocorticoid signaling signature, we compared the differentially regulated mouse genes found in this study to those in an *in vitro* study of human MDA-MB-231 cultured breast cancer cells treated with the synthetic glucocorticoid dexamethasone. Approximately 82% of the differentially expressed 15-week-old mouse mammary gland genes had identifiable

human orthologues and of these genes approximately one fifth were regulated similarly following either exposure to chronic social isolation (mouse mammary gland) or glucocorticoid treatment (human breast cancer cells; see Supplementary Tables S3 and S4 for these gene lists). Given the differences in species, cell types, timing of glucocorticoid exposure, and conditions (*in vivo* versus *in vitro*), this 20% overlap in gene expression suggests that a component of the gene expression differences associated with social isolation may be glucocorticoid-mediated.

The differential gene expression in the early-age mammary glands and the subsequently greater mammary gland tumor growth in isolated versus group-housed mice does not seem to be accompanied by an increased metastatic potential in this model. Although in the isolated mice, tumor sizes were on average larger and the tumor morphology exhibited a trend toward less glandular differentiation, the lack of significant difference in the frequency of microscopic metastases to the lungs suggests that an altered social environment is not associated with the primary metastatic process. One explanation for this finding could be that the specific gene expression pathways (e.g., increased lipid synthesis) that are altered in association with social isolation influence primary mammary gland tumor growth and are distinct from molecular pathways driving metastasis.

In summary, we have used a mouse model of human breast cancer to show for the first time that a chronically isolated social environment correlates with specifically altered mammary gland gene expression. Furthermore, the complement of differentially expressed mammary gland genes associated with social isolation suggests activation of key cancer-linked metabolic pathways. Understanding the specific molecular networks connecting an individual's environment with his or her physiologic stress response and, ultimately, with tissue gene expression favoring tumor growth is expected to uncover novel mechanisms promoting tumor growth in the context of specific environmental stressors. It is possible that the metabolic gene expression pathways identified in this study may also contribute to the mechanisms underlying the observation that patients with self-reported social isolation are at higher risk for diabetes (51) and hypertension (1) as well as cancer (2).

Supplementary Material

Refer to Web version on PubMed Central for supplementary material.

Acknowledgments

References

1. Hawkley LC, Masi CM, Berry JD, Cacioppo JT. Loneliness is a unique predictor of age-related differences in systolic blood pressure. Psychol Aging. 2006; 21:152–64. [PubMed: 16594800]

2. Reynolds P, Kaplan GA. Social connections and risk for cancer: prospective evidence from the Alameda County Study. Behav Med. 1990; 16:101–10. [PubMed: 2224168]

3. Spiegel D, Bloom JR, Kraemer HC, Gottheil E. Effect of psychosocial treatment on survival of patients with metastatic breast cancer. Lancet. 1989; 2:888–91. [PubMed: 2571815]

4. Allegra JC, Lippman ME, Thompson EB, et al. Distribution, frequency, and quantitative analysis of estrogen, progesterone, androgen, and glucocorticoid receptors in human breast cancer. Cancer Res. 1979; 39:1447–54. [PubMed: 427788]

5. Mikosz CA, Brickley DR, Sharkey MS, Moran TW, Conzen SD. Glucocorticoid receptor-mediated protection from apoptosis is associated with induction of the serine/threonine survival kinase gene, sgk-1. J Biol Chem. 2001; 276:16649–54. [PubMed: 11278764]

6. Thaker PH, Han LY, Kamat AA, et al. Chronic stress promotes tumor growth and angiogenesis in a mouse model of ovarian carcinoma. Nat Med. 2006; 12:939–44. [PubMed: 16862152]

7. Palm D, Lang K, Niggemann B, et al. The norepinephrine-driven metastasis development of PC-3 human prostate cancer cells in BALB/c nude mice is inhibited by β-blockers. Int J Cancer. 2006; 118:2744–9. [PubMed: 16381019]

8. McClintock MK, Conzen SD, Gehlert S, Masi C, Olopade F. Mammary cancer and social interactions: identifying multiple environments that regulate gene expression throughout the life span. J Gerontol B Psychol Sci Soc Sci. 2005; 60(Spec No 1):32–41. [PubMed: 15863708]

9. Bartolomucci A, Palanza P, Sacerdote P, et al. Individual housing induces altered immunoendocrine responses to psychological stress in male mice. Psychoneuroendocrinology. 2003; 28:540–58. [PubMed: 12689611]

10. Hermes GL, Rosenthal L, Montag A, McClintock MK. Social isolation and the inflammatory response: sex differences in the enduring effects of a prior stressor. Am J Physiol Regul Integr Comp Physiol. 2006; 290:R273–82. [PubMed: 16210419]

11. Cavigelli SA, Yee JR, McClintock MK. Infant temperament predicts life span in female rats that develop spontaneous tumors. Horm Behav. 2006; 50:454–62. [PubMed: 16836996]

12. Yoshidome K, Shibata MA, Couldrey C, Korach KS, Green JE. Estrogen promotes mammary tumor development in C3(1)/SV40 large T-antigen transgenic mice: paradoxical loss of estrogen receptorα expression during tumor progression. Cancer Res. 2000; 60:6901–10. [PubMed: 11156389]

13. Irizarry RA, Hobbs B, Collin F, et al. Exploration, normalization, and summaries of high density oligo-nucleotide array probe level data. Biostatistics. 2003; 4:249–64. [PubMed: 12925520]

14. Tusher VG, Tibshirani R, Chu G. Significance analysis of microarrays applied to the ionizing radiation response. Proc Natl Acad Sci U S A. 2001; 98:5116–21. [PubMed: 11309499]

15. Wu W, Pew T, Zou M, Pang D, Conzen SD. Glucocorticoid receptor-induced MAPK phosphatase-1 (MPK-1) expression inhibits paclitaxel-associated MAPK activation and contributes to breast cancer cell survival. J Biol Chem. 2005; 280:4117–24. [PubMed: 15590693]

16. Yuan JS, Reed A, Chen F, Stewart CN Jr. Statistical analysis of real-time PCR data. BMC Bioinformatics. 2006; 7:85. [PubMed: 16504059]

17. Zhou XH, Gao S. Confidence intervals for the log-normal mean. Stat Med. 1997; 16:783–90. [PubMed: 9131765]

18. Sahoo S, Brickley DR, Kocherginsky M, Conzen SD. Coordinate expression of the PI3-kinase downstream effectors serum and glucocorticoid-induced kinase (SGK-1) and Akt-1 in human breast cancer. Eur J Cancer. 2005; 41:2754–9. [PubMed: 16246546]

19. Cardiff RD, Anver MR, Gusterson BA, et al. The mammary pathology of genetically engineered mice: the consensus report and recommendations from the Annapolis meeting. Oncogene. 2000; 19:968–88. [PubMed: 10713680]

20. Muglia LJ, Jacobson L, Weninger SC, et al. Impaired diurnal adrenal rhythmicity restored by constant infusion of corticotropin-releasing hormone in corticotropin-releasing hormone-deficient mice. J Clin Invest. 1997; 99:2923–9. [PubMed: 9185516]

21. Green JE, Shibata MA, Yoshidome K, et al. The C3(1)/SV40 T-antigen transgenic mouse model of mammary cancer: ductal epithelial cell targeting with multistage progression to carcinoma. Oncogene. 2000; 19:1020–7. [PubMed: 10713685]

22. Lazarov O, Robinson J, Tang YP, et al. Environmental enrichment reduces Aβ levels and amyloid deposition in transgenic mice. Cell. 2005; 120:701–13. [PubMed: 15766532]

23. Cole SW, Hawkley LC, Arevalo JM, Sung CY, Rose RM, Cacioppo JT. Social regulation of gene expression in human leukocytes. Genome Biol. 2007; 8:R189. [PubMed: 17854483]

24. Pastorino JG, Shulga N, Hoek JB. Mitochondrial binding of hexokinase II inhibits Bax-induced cytochrome c release and apoptosis. J Biol Chem. 2002; 277:7610–8. [PubMed: 11751859]

25. Hatzivassiliou G, Zhao F, Bauer DE, et al. ATP citrate lyase inhibition can suppress tumor cell growth. Cancer Cell. 2005; 8:311–21. [PubMed: 16226706]

26. Brusselmans K, De Schrijver E, Verhoeven G, Swinnen JV. RNA interference-mediated silencing of the acetyl-CoA-carboxylase-α gene induces growth inhibition and apoptosis of prostate cancer cells. Cancer Res. 2005; 65:6719–25. [PubMed: 16061653]

27. Chajes V, Cambot M, Moreau K, Lenoir GM, Joulin V. Acetyl-CoA carboxylase α is essential to breast cancer cell survival. Cancer Res. 2006; 66:5287–94. [PubMed: 16707454]

28. Yancy HF, Mason JA, Peters S, et al. Metastatic progression and gene expression between breast cancer cell lines from African American and Caucasian women. J Carcinog. 2007; 6:8. [PubMed: 17472751]

29. DeBerardinis RJ, Lum JJ, Hatzivassiliou G, Thompson CB. The biology of cancer: metabolic reprogramming fuels cell growth and proliferation. Cell Metab. 2008; 7:11–20. [PubMed: 18177721]

30. Kim JW, Dang CV. Cancer's molecular sweet tooth and the Warburg effect. Cancer Res. 2006; 66:8927–30. [PubMed: 16982728]

31. Arakawa H. Interaction between isolation rearing and social development on exploratory behavior in male rats. Behav Processes. 2005; 70:223–34. [PubMed: 16102906]

32. Ferdman N, Murmu RP, Bock J, Braun K, Leshem M. Weaning age, social isolation, and gender, interact to determine adult explorative and social behavior, and dendritic and spine morphology in prefrontal cortex of rats. Behav Brain Res. 2007; 180:174–82. [PubMed: 17477981]

33. Pang D, Kocherginsky M, Krausz T, Kim SY, Conzen SD. Dexamethasone decreases xenograft response to Paclitaxel through inhibition of tumor cell apoptosis. Cancer Biol Ther. 2006; 5:933–40. [PubMed: 16775428]

34. Sui M, Chen F, Chen Z, Fan W. Glucocorticoids interfere with therapeutic efficacy of paclitaxel against human breast and ovarian xenograft tumors. Int J Cancer. 2006; 119:712–7. [PubMed: 16496381]

35. Draoui A, Vandewalle B, Hornez L, Revillion F, Lefebvre J. β-adrenergic receptors in human breast cancer: identification, characterization and correlation with progesterone and estradiol receptors. Anticancer Res. 1991; 11:677–80. [PubMed: 1648332]

36. Weaver IC, Cervoni N, Champagne FA, et al. Epigenetic programming by maternal behavior. Nat Neurosci. 2004; 7:847–54. [PubMed: 15220929]

37. Burkhart BA, Ivey ML, Archer TK. Long-term low level glucocorticoid exposure induces persistent repression in chromatin. Mol Cell Endocrinol. 2009; 298:66–75. [PubMed: 19007849]

38. Pedersen PL, Mathupala S, Rempel A, Geschwind JF, Ko YH. Mitochondrial bound type II hexokinase: a key player in the growth and survival of many cancers and an ideal prospect for therapeutic intervention. Biochim Biophys Acta. 2002; 1555:14–20. [PubMed: 12206885]

39. Mathupala SP, Ko YH, Pedersen PL. Hexokinase II: cancer's double-edged sword acting as both facilitator and gatekeeper of malignancy when bound to mitochondria. Oncogene. 2006; 25:4777–86. [PubMed: 16892090]

40. Bustamante E, Pedersen PL. High aerobic glycolysis of rat hepatoma cells in culture: role of mitochondrial hexokinase. Proc Natl Acad Sci U S A. 1977; 74:3735–9. [PubMed: 198801]

41. Pedersen PL. Warburg, me and Hexokinase 2: Multiple discoveries of key molecular events underlying one of cancers' most common phenotypes, the "Warburg Effect", i.e., elevated glycolysis in the presence of oxygen. J Bioenerg Biomembr. 2007; 39:211–22. [PubMed: 17879147]

42. Tong L. Acetyl-coenzyme A carboxylase: crucial metabolic enzyme and attractive target for drug discovery. Cell Mol Life Sci. 2005; 62:1784–803. [PubMed: 15968460]

43. Swinnen JV, Brusselmans K, Verhoeven G. Increased lipogenesis in cancer cells: new players, novel targets. Curr Opin Clin Nutr Metab Care. 2006; 9:358–65. [PubMed: 16778563]

44. Milgraum LZ, Witters LA, Pasternack GR, Kuhajda FP. Enzymes of the fatty acid synthesis pathway are highly expressed in in situ breast carcinoma. Clin Cancer Res. 1997; 3:2115–20. [PubMed: 9815604]

45. Beckers A, Organe S, Timmermans L, et al. Chemical inhibition of acetyl-CoA carboxylase induces growth arrest and cytotoxicity selectively in cancer cells. Cancer Res. 2007; 67:8180–7. [PubMed: 17804731]

46. Brunet J, Vazquez-Martin A, Colomer R, Grana-Suarez B, Martin-Castillo B, Menendez JA. BRCA1 and acetyl-CoA carboxylase: the metabolic syndrome of breast cancer. Mol Carcinog. 2008; 47:157–63. [PubMed: 17620310]

47. Travers MT, Barber MC. Insulin-glucocorticoid interactions in the regulation of acetyl-CoA carboxylase-α transcript diversity in ovine adipose tissue. J Mol Endocrinol. 1999; 22:71–9. [PubMed: 9924182]

48. Bujalska IJ, Hewitt KN, Hauton D, et al. Lack of hexose-6-phosphate dehydrogenase impairs lipid mobilization from mouse adipose tissue. Endocrinology. 2008; 149:2584–91. [PubMed: 18218694]

49. Couto RC, Couto GE, Oyama LM, Damaso AR, Silveira VL, Nascimento CM. Effect of adrenalectomy and glucocorticoid therapy on lipid metabolism of lactating rats. Horm Metab Res. 1998; 30:614–8. [PubMed: 9851668]

50. Andersen BL, Yang HC, Farrar WB, et al. Psychologic intervention improves survival for breast cancer patients: a randomized clinical trial. Cancer. 2008; 113:3450–8. [PubMed: 19016270]

51. Maty SC, Lynch JW, Raghunathan TE, Kaplan GA. Childhood socioeconomic position, gender, adult body mass index, and incidence of type 2 diabetes mellitus over 34 years in the Alameda County Study. Am J Public Health. 2008; 98:1486–94. [PubMed: 18556612]
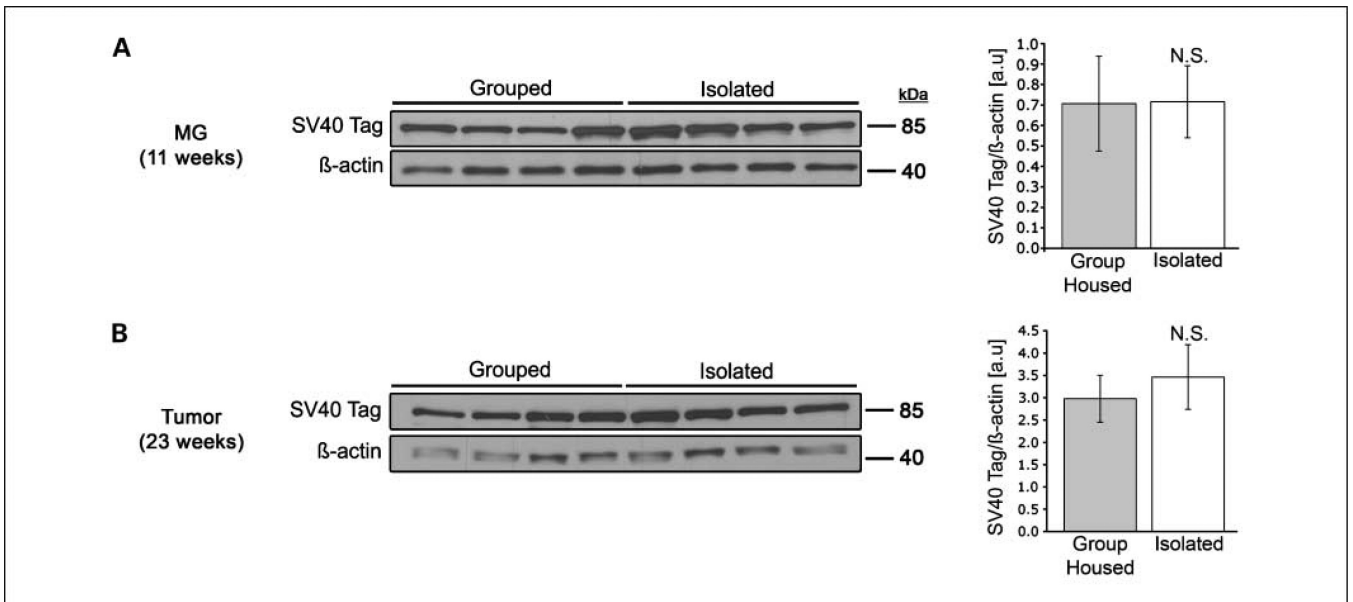
Fig. 1.
Differences in SV40 Tag expression are not associated with the social environment. (*A*) Isolated (*n* = 4) and group-housed (*n* = 4) mouse mammary glands (*MG*; 11 wk) or (*B*) tumors (23 wk) were collected and prepared for Western analysis. Proteins were resolved by SDS-PAGE, and SV40 Tag expression was examined. β-Actin was probed as a loading control. Molecular weight markers are shown. Densitometry is shown on the right as the mean value +/− SEM (error bars). N.S. = non-significant difference.
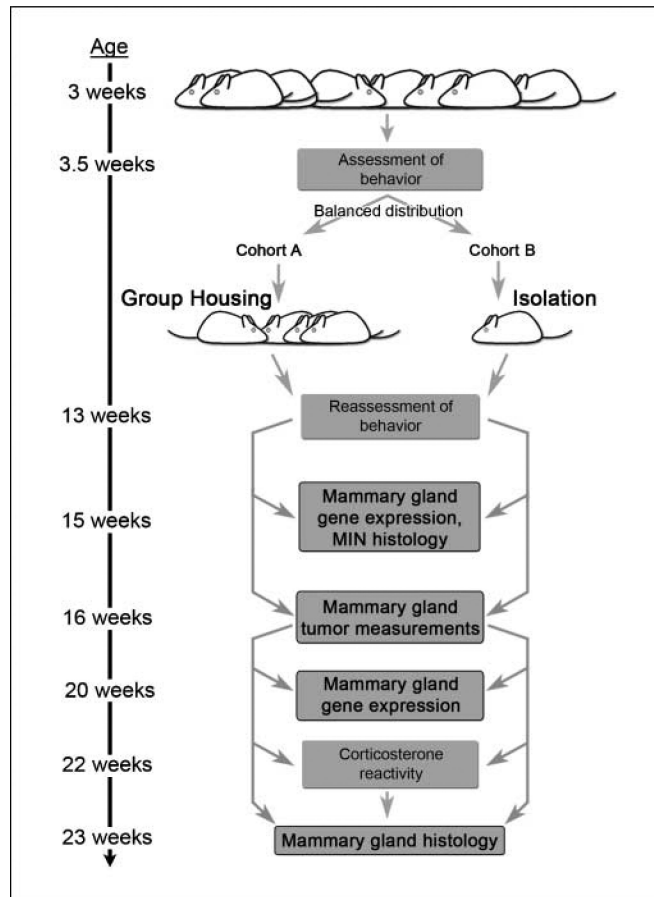
Fig. 2.
Experimental schema. Female C3 (1)/SV40 Tag mice were weaned from their mothers at 3 wk of age; behavior was assessed using a standard open-field test (see Materials and Methods). Based on the results of this initial open-field testing, the mice were divided into two cohorts with a balanced distribution of behavior: *cohort A*, group-housed cohort (four mice per cage); *cohort B*, individually housed cohort. At 13 wk of age, behavior testing was repeated. At 15 wk of age, global gene expression in the mammary glands of a subset of isolated versus group-housed mice was determined. Beginning at 16 wk, mammary gland tumor volumes were measured weekly in both cohorts. At 20 wk, gene expression was evaluated in a second subset of mice, and at 22 wk serum corticosterone reactivity in response to a mild, acute stressor was measured. Mice were then sacrificed and mammary glands were weighed and the pathology was examined.
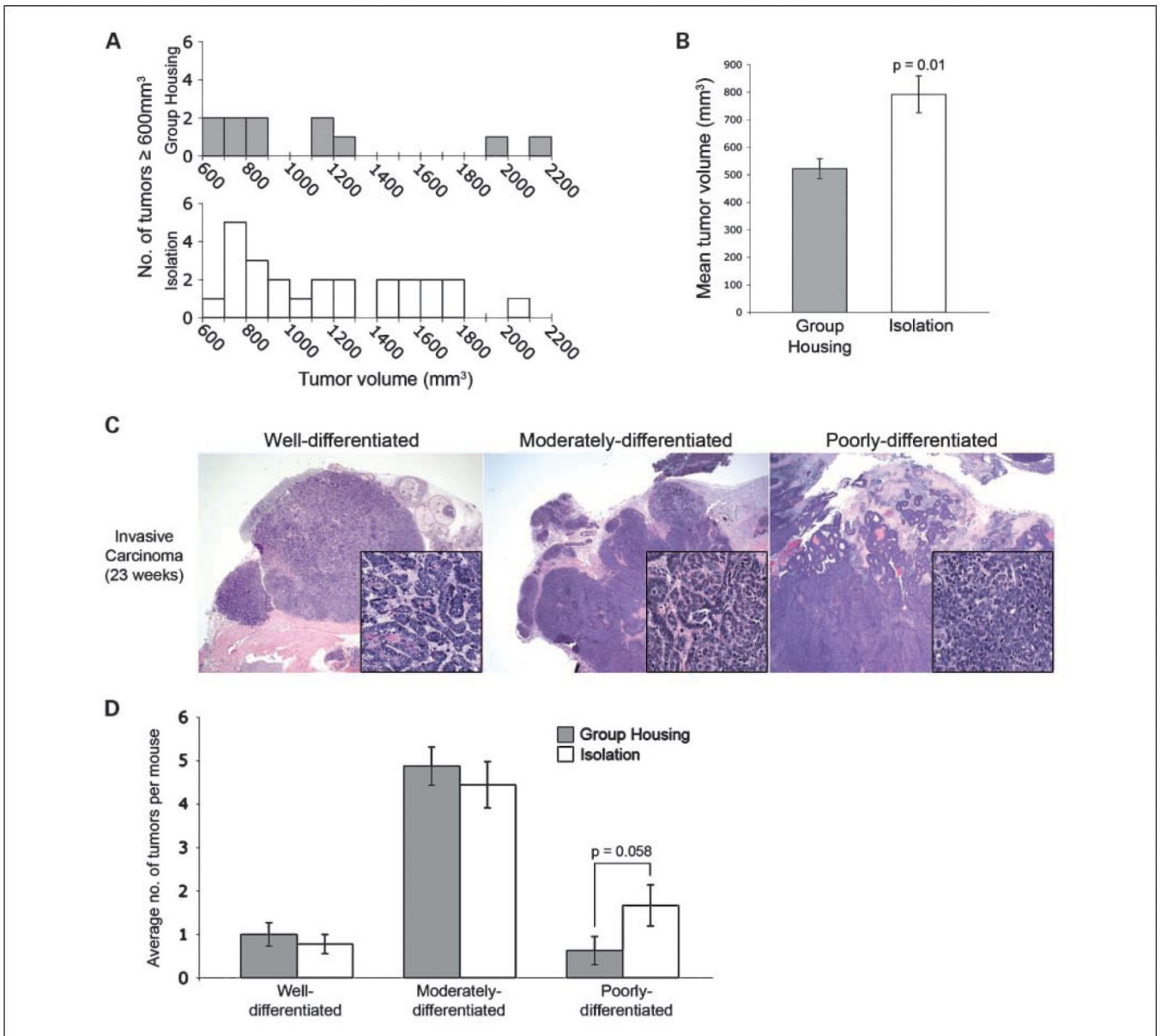
Fig. 3.

Socially isolated SV40 Tag mice develop significantly larger mammary gland tumors. *A,* the distribution of tumor volumes ≥ 600 mm^3 from grouped (*gray columns*) versus isolated (*white columns*) mice. *B,* isolated mice had overall significantly larger mean tumor volume at 21 wk of age. Mean tumor volume represents the least-square means as determined using the mixed-effects ANOVA model (*, $P = 0.01$ based on mixed-effects ANOVA). *C,* representative examples of poorly, moderately, and well-differentiated mammary carcinomas from 23-wk-old transgenic mice (H&E, 12.5×, inset 400×). *D,* isolated animals exhibit a trend toward a higher number of poorly differentiated tumors per mouse (Error bars = SEM, $P = 0.058$ based on Poisson regression).
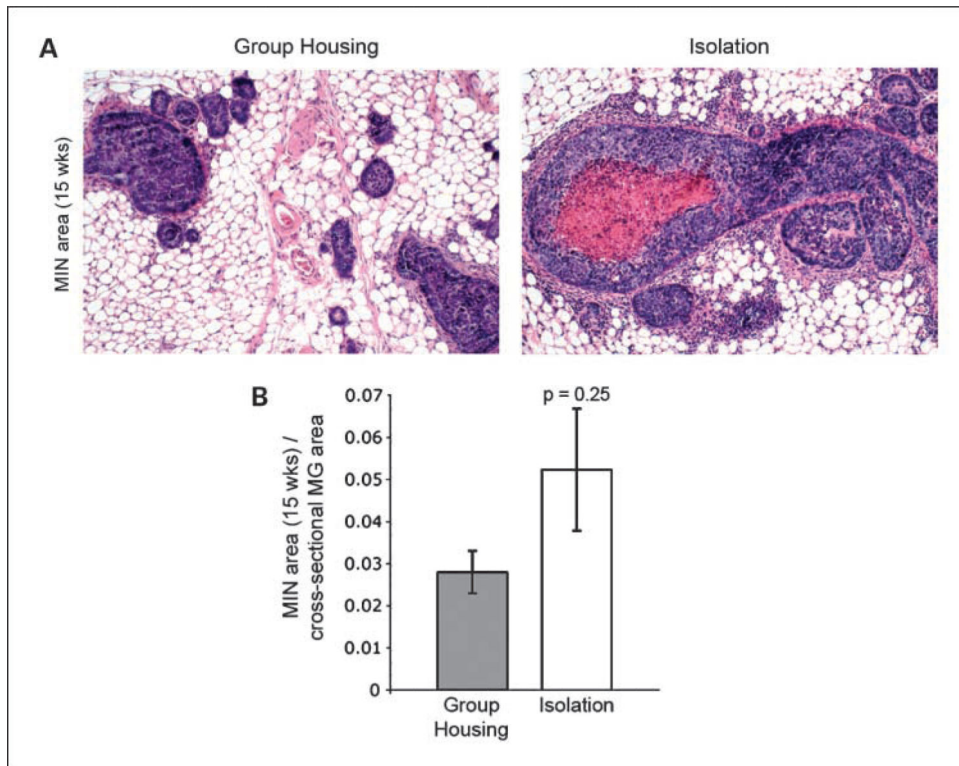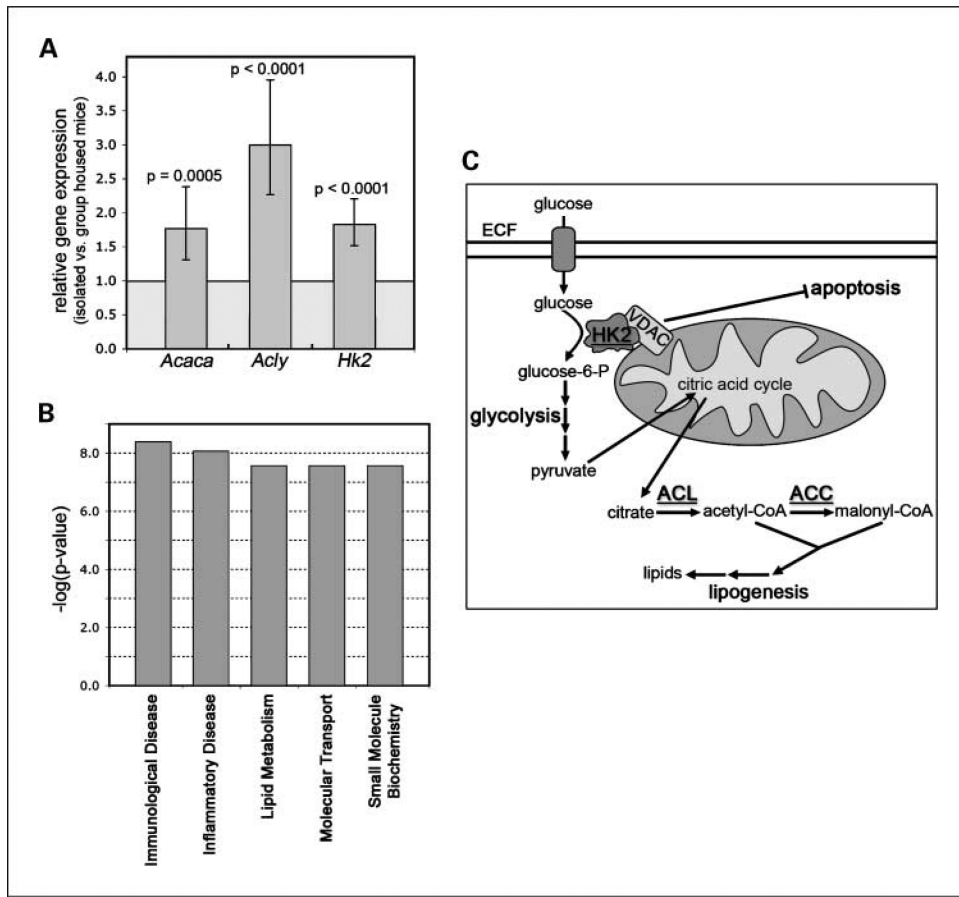
Fig. 4.
Mammary glands from isolates trend toward a greater MIN area. *A,* representative sections of MIN in mammary glands from group-housed (*left*) versus isolated (*right*) mice at 15 wk of age (H&E, 100×). *B,* the average mammary gland area occupied by MIN is greater in the isolated versus group-housed animals ($n = 4$, $n = 4$, Error bars = SEM, $P = 0.25$ based on Wilcoxon rank-sum test).

Fig. 5.
Chronic social isolation–associated mammary gland gene expression. *A,* validation of individual gene expression. Quantitative RT-PCR values are given as fold change relative to expression in group-housed mice (*n* = 4 individual mice per cohort). Differences in expression were found to be significant based on the Ct method estimates using a mixed-effects ANOVA model (Error bars = SEM, *Acaca, P* = 0.0005; *Acly, P* < 0.0001; *Hk2, P* < 0.0001). *B,* the top functional gene categories associated with social isolation based on mammary gland gene expression differences at 15 wk were identified using the IPA 6.5 software. *C,* human *HK2* (hexokinase 2), *ACL* (ATP citrate lyase), and *ACC* (acetyl-CoA carboxylase α) genes encode key components of cancer-associated glycolysis and lipogenesis pathways.
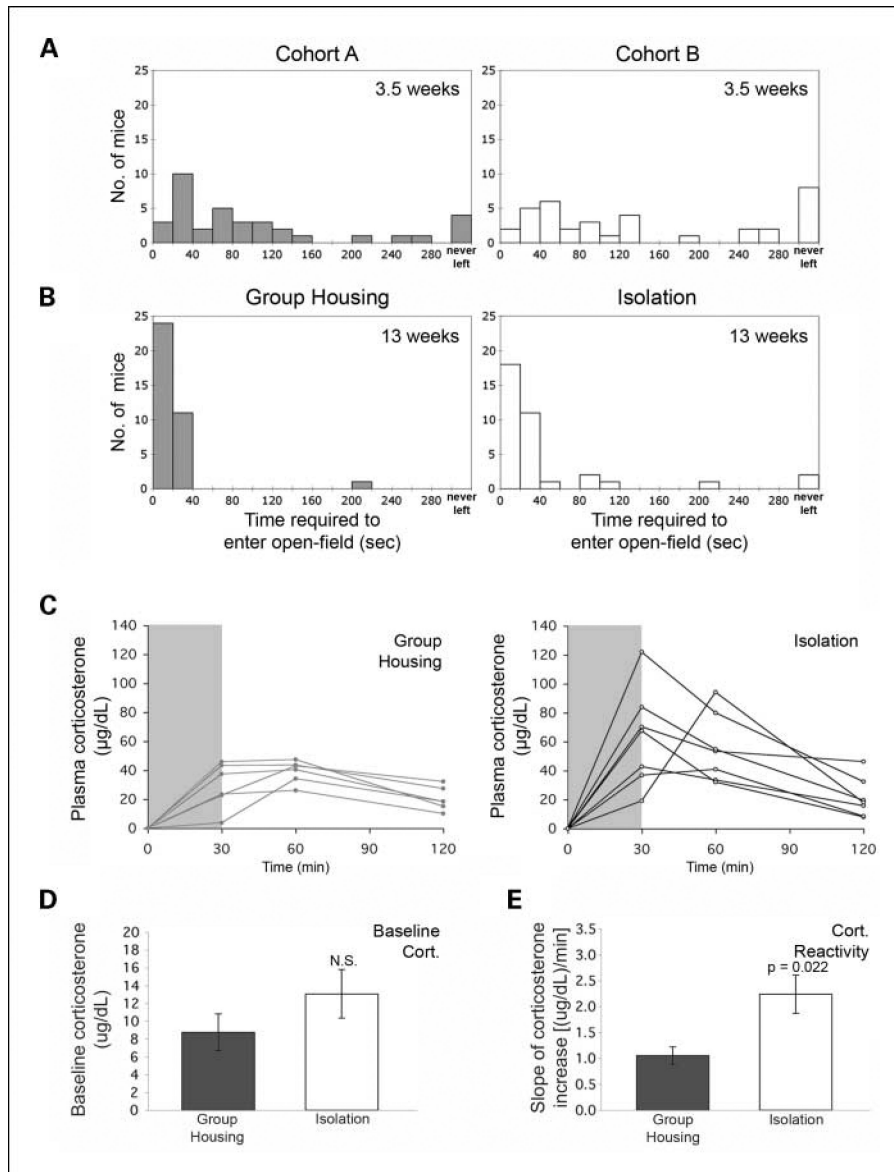
Fig. 6.

Mice subjected to social isolation exhibit increased vigilance and higher corticosterone reactivity. *A,* before separation into grouped or isolated housing conditions, innate vigilance was evaluated by measuring the time (in seconds) it took for each mouse to venture into the open field. Based on these measurements, mice were then separated into two cohorts (*cohort A* and *cohort B*) with a balanced distribution of vigilance; cohort A was then group-housed and cohort B was individually housed. *B,* following 9.5 wk of either group housing or isolation, behavioral testing was repeated. Overall, isolated animals displayed more vigilant behavior; that is, significantly longer times to enter an open-field compared with group-housed mice ($P = 0.018$ based on log-rank test). *C,* at 22 wk of age, the reactive stress response was assessed ($n = 6$ group-housed, $n = 7$ isolated) by measuring serum corticosterone levels before and following a 30-min mild restraint stressor; individual corticosterone levels over time (relative to baseline) are shown. *Gray shading,* the duration

of restraint. *D,* no significant difference (*N.S.*) was found in baseline serum corticosterone levels. *Error bars,* SEM. *E,* isolated mice exhibit significantly increased corticosterone reactivity. The slope of the increase (reactivity) was determined by calculating the difference between the baseline and highest level for each animal divided by the time elapsed. *Error bars,* SEM ($P = 0.022$ based on the Mann-Whitney *U* test).